PB81-222713

Response of Lead Solubility to Dissolved Carbonate in Drinking Water

(U.S.) Municipal Environmental Research Lab.
Cincinnati, OH

1980

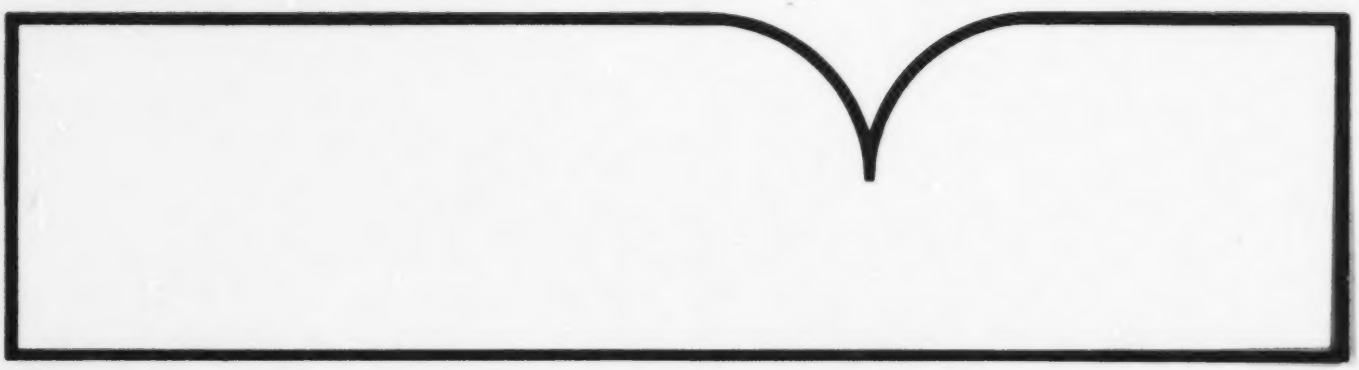

U.S. Department of Commerce
National Technical Information Service
NTIS

TECHNICAL REPORT DATA
(Please read Instructions on the reverse before completing)

1. REPORT NO.	2.	3. RE PB81-222713
EPA-600/J-80-294	ORD Report	

4. TITLE AND SUBTITLE
Response of Lead Solubility to Dissolved Carbonate In Drinking Water

5. REPORT DATE
June 1981

6. PERFORMING ORGANIZATION CODE

7. AUTHOR(S)
Michael R. Schock

8. PERFORMING ORGANIZATION REPORT NO.

9. PERFORMING ORGANIZATION NAME AND ADDRESS
Drinking Water Research Division
Municipal Environmental Research Laboratory, U.S. EPA,
26 W. St. Clair Street
Cincinnati, Ohio 45268

10. PROGRAM ELEMENT NO.

11. CONTRACT/GRANT NO.

12. SPONSORING AGENCY NAME AND ADDRESS
Municipal Environmental Research Laboratory - Cin., OH
Office of Research and Development
U. S. Environmental Protection Agency
Cincinnati, Ohio 45268

13. TYPE OF REPORT AND PERIOD COVERED
Journal Article

14. SPONSORING AGENCY CODE
EPA.600/14

15. SUPPLEMENTARY NOTES
Published in Jour. Amer. Water Works Assn., 72:12:695 (Dec. 1980); erratum, March, 1981 p.36.

16. ABSTRACT

A model is presented showing the detailed response of the theoretical solubility curves for lead to changes in dissolved inorganic carbonate concentration (TIC) and pH at 25°C. Aqueous Pb(II) ion, lead carbonate complexes, lead hydroxide monomers and polymers, and the solids lead hydroxide, cerussite and hydrocerussite were considered.

Results of pipe loop solubility experiments at log TIC(mol/L) values of -3.6, -3.0 and -2.7 (25, 100 and 200 mg/L as $CaCO_3$) are presented. The model agrees very well with these data, as well as with previously published pipe coupon tests and precipitation data at high TIC.

The predicted minimum molar solubility of lead is shown to increase by a factor of approximately 2 to 10,000 over that predicted by previous two-solid phase models that ignored lead carbonate complexes. Further, a general reversal in trend occurs with increasing TIC and curve shapes are greatly changed in contrast with those previous models.

Reduction of lead levels to below 0.05 mg/L in standing samples purely by hydroxide and carbonate solubility considerations is possible, but only under very restricted pH and TIC conditions.

17. KEY WORDS AND DOCUMENT ANALYSIS

a. DESCRIPTORS	b. IDENTIFIERS/OPEN ENDED TERMS	c. COSATI Field/Group
Corrosion, Corrosion Products, Chemical equilibrium, Potable Water, Lead, Solubility, Computer modelling, Chemical speciation		

PRODUCT OF:
NATIONAL TECHNICAL INFORMATION SERVICE
U.S. DEPARTMENT OF COMMERCE
SPRINGFIELD, VA. 22161

18. DISTRIBUTION STATEMENT	19. SECURITY CLASS *(This Report)*	21. NO. OF PAGES
Can be freely distributed.	20. SECURITY CLASS *(This page)*	22. PRICE

EPA-600/J-80-294
Journal Article

One of the solvents found in widely used coatings is tetrachloroethylene, an undesirable drinking water contaminant. Its detection in one of EBMUD's new reservoirs led to valving off the reservoir to see how high the concentration would go—it peaked at 930 μg/L.

It has been known for many years[1] that redwood supports the growth of coliform organisms, but it has not generally been recognized that many coating materials are also growth supporting. The Thames River Authority (TRA) of England routinely tests jointing materials, sealants, and coatings for bacterial growth support, using Thames River water for the inoculum.[2] The authority reports "... most of the solvent-based paints and protective coatings supported growth whilst the epoxy coatings and bituminous paints which had been well cured were mostly satisfactory." Although EBMUD's testing results do not completely support TRA's comment on the effect of curing, the results do confirm the capacity of some coatings and materials to support growth to a significant and unacceptable degree, independent of any other source of nutrients.

Presumably every water bacteriologist has encountered circumstances under which the continued presence of coliforms had no ready explanation. The source of at least some unexpectedly high concentrations of coliforms has been demonstrated by the EBMUD investigations and should be of interest to water purveyors who use coatings in the interior of treated water tanks.

Acknowledgments

The original demonstration that the source of the high bacterial counts in the cited reservoir was the interior coating was made by R. B. Baker, former senior chemist of the East Bay Municipal Utility District. The authors are grateful for the cooperative effort of Ramon Seidler and Thomas Evans of the department of microbiology of Oregon State University in corroborating the work reported here. Provided with three blind samples, they confirmed the authors' results on two of the coating samples. The third coating is still under investigation for a recognized but as yet unexplained contamination.

References

1. Jones, F.E. & Greenburg, A.E. Coliform Bacteria in Redwood Storage Tanks. *Jour. AWWA*, 56:11:1489 (Nov. 1964).
2. Burman, N.P. & Colbourne, J.S. Techniques for the Assessment of Growth of Microorganisms on Plumbing Materials Used in Contact with Potable Water Supplies. *Jour. Applied Bact.*, 43:1:137 (1977).

A paper contributed to and selected by the JOURNAL, authored by William M. Eligas (Active Member, AWWA), chemist II, and Raymond Lee (Active Member, AWWA), senior chemist, both of the water quality laboratory, East Bay Municipal Utility District, Oakland, Calif.

65504 4120, 5300

A detailed protocol for the testing procedure used in this study is available upon request from the authors, who stress that extreme care should be used in performing the tests so as to avoid spurious results due to contamination. Requests should be sent to William M. Eligas, Water Quality Laboratory, East Bay Municipal Utility District, 7700 Greenly Dr., Oakland, Calif. 94605.

Response of lead solubility to dissolved carbonate in drinking water

Michael R. Schock

Because of the potential toxicity of lead and its deleterious effects on human health, increased attention has been given to the use of lead piping materials in household plumbing. Water that is corrosive to lead has been observed to leach considerable amounts of lead from pipes, especially after the water has been standing in the pipes for several hours. This paper presents a revised model showing the detailed response of the theoretical solubility curves for lead to changes in dissolved inorganic carbonate concentration (C_t) and pH at 25° C. The model agrees well with previously published pipe loop solubility experimental data as well as with pipe coupon tests and precipitation data at high C_t.

Lead pipe is still in fairly widespread use in household plumbing systems. Zoetman and Haring[1] report that in Belgium, France, the Irish Republic, and the United Kingdom over 37 percent of the total plumbing materials in use for water distribution in houses is lead. Many areas of the US, particularly New England, also use lead piping material. Water that is corrosive to lead has been observed to leach considerable amounts of lead from the pipes, especially while standing for several hours or more, and this has created considerable concern because of its potential toxicity and other health effects in humans.[2,3]

In view of this concern and the mixed success found with several modes of water treatment within the distribution system to control the corrosivity of the water towards lead pipe,[3] research has been undertaken by the Drinking Water Research Division (DWRD) of the US Environmental Protection Agency (US EPA) to investigate some treatment methodologies that might facilitate compliance with the National Interim Primary Drinking Water Regulations (NIPDWR), which specify a maximum contaminant level (MCL) of 0.05 mg/L for total lead.[4] This paper focuses on considerations relating to pH and total inorganic carbonate control as a means of minimizing corrosion by the precipitation of a lead carbonate, hydroxycarbonate, or hydroxide film.

A model is presented showing the detailed response of the theoretical solubility curves for lead to changes in dissolved inorganic carbonate concentration (C_t) and pH at 25°C. Considered were lead carbonate complexes, lead hydroxide monomers and polymers, the solids $Pb(OH)_2$, $PbCO_3$, and $Pb_3(OH)_2(CO_3)_2$, and the free Pb(II) ion.

Results of pipe loop solubility experiments at C_t values of $10^{-3.6}$, $10^{-3.0}$, and $10^{-2.7}$ M (25, 100, and 200 mg/L as $CaCO_3$) are presented. The model agrees very well with these data, as well as with previously published pipe coupon tests and precipitation data at high C_t.

The predicted minimum molar solubility of lead is increased by a factor of $\sim 10^{0.3}$ to 10^4 over that suggested by previous two solid phase models ignoring lead carbonate complexes. Further, a general reversal in trend occurs with increasing C_t and curve shapes are greatly changed in contrast with those previous models.

Reduction of lead levels to below 0.05

TABLE 1

*Standard Gibbs free energies of formation of lead and related species at 25° C**

Species	ΔG_f° kcal/mole	Source
PbO, red, solid	−45.06	1
PbO, yellow, solid	−44.81	1
PbO_2, solid	−51.97	2
Pb_3O_4, solid	−143.71	3
$Pb(OH)_2$, fresh ppt.	−101.3	4
$Pb(OH)_2$, aged	−108.0	5
$PbCO_3$, solid	−149.8	6
$Pb_3(OH)_2(CO_3)_2$, solid	−408.6	7
Pb^{2+}	−5.73	8
$PbOH^+$	−52.57	9
$Pb(OH)_2^0$	−96.04	9
$Pb(OH)_3^-$	−137.5	9
Pb_2OH^{3+}	−50.47	10
$Pb_3(OH)_4^{2+}$	−211.4	10
$Pb_4(OH)_4^{4+}$	−221.2	10
$Pb_6(OH)_8^{4+}$	−428.4	10
$PbCO_3^0$	−141.6	11
$Pb(CO_3)_2^{2-}$	−272.2	11
H_2O	−56.690	12
OH^-	−37.604	12
$H_2CO_3^*$	−148.95	13
HCO_3^-	−140.28	13
CO_3^{2-}	−126.19	14
CO_2, gas	−94.257	12

*All species are aqueous unless otherwise stated.

TABLE 1A

Sources of ΔG_f° data

1. Recalculated from Wagman, D.D. et al (1968). Selected values of chemical thermodynamic properties from National Bureau of Standards Technical Note 270-3, using ΔG_f° calculated from that compilation for the reaction $Pb^{2+} + H_2O = PbO + 2H^+$ with ΔG_f° Pb^{2+} and ΔG_f° H_2O given here.
2. Same as source 1 but using only ΔG_f° H_2O from this list for the reaction $Pb^{2+} + 2H_2O = PbO_2 + 2H^+ + 2e^-$
3. Same as source 2, for the reaction $3Pb^{2+} + 4H_2O = Pb_3O_4 + 8H^+ + 8e^-$
4. Calculated from $\log K_{sp} = -14.93$; given in Barć, A.J. *Chemical Equilibrium*, Harper and Row, New York (1966). Values of ΔG_f° for OH^- and Pb^{2+} were taken from this table.
5. Recalculated from Wagman, D.D., et al (1968). Selected values of chemical thermodynamic properties from National Bureau Bureau of Standards Technical Note 270-3, using the original ΔG_f° corrected for the new values for ΔG_f° OH^- and Pb^{2+}.
6. Calculated from $\log K_{sp} = -13.13$ quoted in Hem, J.D. (19--) *Geochim. Cosmochim. Acta.* 40:599, using ΔG_f° for Pb^{2+} and CO_3^{2-} from this listing.
7. Calculated from $\log K = 5.10$ for the reaction $3Pb(OH)_2 + 2CO_3^{2-} = Pb_3(OH)_2(CO_3)_2 + 2OH^-$ cited in Baes, C.F. and Mesmer, R. *The Hydrolysis of Cations*, John Wiley and Sons, New York (1976). Values of ΔG_f° for $Pb(OH)_2$, OH^-, and Pb^{2+} are from this table.
8. Calculated using values of S°_{298} and $\Delta H_f^\circ{}_{298}$ to obtain $\Delta G^\circ_{f\,298}$ Pb^{2+} indirectly through the reaction $Pb^0 + 2H^+ = Pb^{2+} + H_2$ and the relationships $\Delta G_R^\circ = \Delta H_R^\circ - T\Delta S$, and 1.0 thermochemical calorie = 4.184 joules. Data from *Jour. Chem. Thermodynamics.*, 9:705 (1977).
9. Derived from cumulative formation constants at zero ionic strength given by Lind, C.J., *Environ. Sci. Technol.*, 12:1406, (1978), using ΔG_f° for Pb^{2+} and OH^- listed here.
10. Calculated from hydrolysis constants tabulated in Baes, C.F. and Mesmer, R. (1976) op. cit., using ΔG_f° for Pb^{2+} and H_2O tabulated here.
11. Calculated from average of concentration constants given for $I = 0.1$ by Bilinski, H. et al *Anal. Chim. Acta*, 84:157 (1976). Using the Davies equation for activity coefficients of charge species and $\log f = -0.5$ for $PbCO_3^0$ gives $\log \beta_{,,} = 7.06$ and $\log \beta_{,,} = 10.31$. ΔG_f° Pb^{2+} and ΔG_f° CO_3^{2-} from this listing were then used to obtain ΔG_f° $PbCO_3^0$ and ΔG_f° $Pb(CO_3)_2^{2-}$
12. Parker, V.B. et al. Selected Thermochemical Data Compatible with the CODATA Recommendations. NBSIR75-968, US National Bureau of Standards (1978).
13. Calculated from temperature functions of the equilibrium constants for the reactions CO_2 (g) + $H_2O = H_2CO_3^*$ and $H_2CO_3^* = HCO_3^- + H^+$ using these values of ΔG_f° CO_2 (g) and H_2O and regression coefficients obtained by Harned, H. S. and Davies, R. Jr. *Jour. Amer. Chem. Soc.*, 65:2030 (1943).
14. Calculated from the $\log K$ versus T function given by Harned, H. S. and Scholes, S. R. Jr. *J. Amer. Chem. Soc.*, 63:1706 (1941), using values of ΔG_f° H_2O given here and the previously stated derived value of ΔG_f° HCO_3^-.

mg/L in standing samples purely by hydroxide and carbonate solubility considerations is possible, but only under very restricted conditions, an important consideration when attempting to control lead concentrations.

Previous solubility models

Solubility models for lead in a carbonate-containing aqueous system have been suggested as a basis both for lead removal at the treatment plant[5,6] and for limiting lead concentrations in the distribution system itself.[7,8] The dominant feature of three of these particular models is the prediction of maintaining lead solubility below the NIPDWR-specified MCL of 0.05 mg/L as a simple function of total dissolved carbonate concentration (C_t) and pH.[5-7]

Hem and Durum[5] considered the solid phases $Pb(OH)_2$, $PbCO_3$ (cerussite), and $Pb_3(OH)_2(CO_3)_2$ (hydrocerussite), along with the aqueous lead species Pb^{2+}, $PbOH^+$, $PB(OH)_2^0$, and $Pb(OH)_3^-$, at C_t from $10^{-4.97}$ M to 10^{-2} M (1.4 to 1000 mg/L as $CaCO_3$) and at ionic strengths of 0.1 and infinite dilution. They concluded that hydrocerussite had such a short stability range (pH ~ 7.5 to pH ~ 8.5) that it could be neglected without serious error. The temperature was assumed to be 25°C.

Patterson et al[6] produced a similar model (at zero ionic strength only) that was compared to laboratory precipitation data at initial C_t values of $10^{-3.6}$, $10^{-2.7}$, and $10^{-1.1}$ M (25, 200, and 7950 mg/L as $CaCO_3$). The main difference between this model and that of Hem and Durum[5] was the choice of the solubility constant K_{so} for the reaction

$$Pb(OH)_2(s) = Pb^{2+} + 2\ OH^-$$

where s indicates a solid phase.

The value chosen by Patterson et al[6] of $10^{-14.9}$ can be compared to that of Hem and Durum[5] by using the standard Gibbs free energies of formation table of the latter, ΔG_f° for OH^- from a compatible source[9] (−37.594 kcal/mole) and the relationships[10] (at 25°C)

$$\Delta G_R^\circ = \Sigma \Delta G_f^\circ \text{ products} - \Sigma \Delta G_f^\circ \text{ reactants} \quad (1)$$

$$\log K = \Delta G_R^\circ / -1.364 \quad (2)$$

This gives a value for K_{so} (as written) of $10^{-10.85}$, which is probably unreasonably small for a fresh natural precipitate. Choosing the Gibbs free energy value for $Pb(OH)_2$(s) of −108.1 kcal/mole dictated the conclusion of Hem and Durum[5] that hydrocerussite occupies a very limited stability field, when, in fact, hydrocerussite is probably the thermodynamically stable phase over much of the pH region from approximately 7 to more than 12 based on other solubility and thermodynamic data. Therefore, the literature value of K_{so} chosen by Patterson et al[6] is probably more correct. Patterson et al[6] also suggested that a better fit to their data might be obtained by considering the solid $Pb_3(OH)_2(CO_3)_2$ in the model, but they did not include it at that time.

The model presented by O'Brien[7] contained little background information on the species considered or the thermodynamic assumptions and data employed. It is assumed to be equivalent to that of Patterson et al.[6]

By stipulating the total concentration of dissolved carbonate species and prohibiting exchange with atmospheric CO_2 gas, a closed system[10,11] can be defined, as was done by Patterson et al,[6] Patterson and O'Brien,[8] and Hem and Durum[5] in the cases compared here. For precipitation experiments open to the atmosphere this would be technically incorrect. However, because of the slow rate of hydration of CO_2 gas, the high pH necessary to substantially exceed the initial C_t of the experiments discussed,[6] and the comparatively short retention times of the sludges involved, this is generally a good approximation. Some behavioral deviation is seen, however, from that of a strictly closed system, in the Patterson et al[6] data.

More recently, models have been independently developed[8,12,13] that include the third solid, $Pb_3(OH)_2(CO_3)_2$, and also the aqueous complexes $PbCO_3^0$ and $Pb(CO_3)_2^{2-}$. Including these complexes, the existence of which has been well documented in the literature,[14-19] considerably complicates the response of the total dissolved lead concentration to concentration changes of inorganic carbonate and the hydrogen ion. One of the purposes of this paper is to provide an elucidation of this relationship, also taking into account ionic strength. The predictions of this model are then compared to laboratory precipitation data,[6] coupon tests,[8] some field data,[3,13] and some new pipe loop solubility experiments.

Theoretical considerations

The solubility model. The first step was

TABLE 2
Calculated formation constants of complexes of Pb(II) at 25°C

Reaction	Name of Constant	Log β
$Pb^{2+} + OH^- \rightleftarrows PbOH^+$	β_{11}	6.77
$Pb^{2+} + 2OH^- \rightleftarrows Pb(OH)_2^0$	β_{12}	11.07
$Pb^{2+} + 3OH^- \rightleftarrows Pb(OH)_3^-$	β_{13}	13.90
$2Pb^{2+} + OH^- \rightleftarrows Pb_2OH^{3+}$	β_{21}	7.63
$3Pb^{2+} + 4OH^- \rightleftarrows Pb_3(OH)_4^{2+}$	β_{34}	32.10
$4Pb^{2+} + 4OH^- \rightleftarrows Pb_4(OH)_4^{4+}$	β_{44}	35.00
$6Pb^{2+} + 8OH^- \rightleftarrows Pb_6(OH)_8^{4+}$	β_{68}	68.31
$Pb^{2+} + CO_3^{2-} \rightleftarrows PbCO_3^0$	β_{c11}	7.10
$Pb^{2+} + 2CO_3^{2-} \rightleftarrows Pb(CO_3)_2^{2-}$	β_{c12}	10.33

TABLE 3
Other calculated equilibrium constants used in this model at 25°C

Reaction	Constant	Log K
$Pb(OH)_2$ fresh $\rightleftarrows Pb^{2+} + 2OH^-$	K_{sp}	−14.93
$Pb(OH)_2$ aged $\rightleftarrows Pb^{2+} + 2OH^-$	K_{sp}	−19.85
$PbCO_3$ solid $\rightleftarrows Pb^{2+} + CO_3^{2-}$	K_{sp}	−13.11
$Pb_3(OH)_2(CO_3)_2$ solid $\rightleftarrows 3\,Pb^{2+} + 2OH^- + 2CO_3^{2-}$	K_{sp}	−46.78
$H_2O + CO_2\,(g) \rightleftarrows H_2CO_3^*$	K_H	− 1.46*
$H_2CO_3^* \rightleftarrows HCO_3^- + H^+$	K_1	− 6.35*
$HCO_3^- \rightleftarrows CO_3^{2-} + H^+$	K_2	−10.33†
$H_2O \rightleftarrows OH^- + H^+$	K_W	−13.99

*Directly from equations given by Harned, H.S. & Davis, R. Jr. *Jour. Amer. Chem. Soc.*, 65:2030 (1943).
†Directly from equation given by Harned, H.S. & Scholes, S.R. Jr. *Jour. Amer. Chem. Soc.*, 63:1706 (1941).

establishment of an internally consistent set of standard Gibbs free energies of formation, to be used both here and in potential–pH equilibrium diagram calculations. These data are summarized in Table 1. Because of rounding errors, the equilibrium constants calculated by these values plus Eq (1) and (2) may differ from the originals, but the precision is considered to be well within the probable uncertainties of the Ks themselves. Tables 2 and 3 give the critically evaluated equilibrium constants used herein, as calculated using the Gibbs free energy values of Table 1 plus Eq (1) and (2) derived from manipulations of the given equations and constants for internal consistency.

The total solubility of Pb(II), S_t, is given for this model by the mass balance equation

$$S_t = [Pb^{2+}] + [PbOH^+] + [Pb(OH)_2^0] + [Pb(OH)_3^-] + 2[Pb_2OH^{3+}] + 3[Pb_3(OH)_4^{2+}] + 4[Pb_4(OH)_4^{4+}] + 6[Pb_6(OH)_8^{4+}] + [PbCO_3^0] + [Pb(CO_3)_2^{2-}] \quad (3)$$

where brackets indicate molar concentration.

In solution, the activity of specie i is defined as the product of its molar concentration $[i]$ and activity coefficient f_z

$$ai = [i]f_z$$

Activity coefficients were calculated for charged species (of charge z) through the Davies equation[11,20]

$$\log f_z = -Az^2\left[\frac{\sqrt{I}}{1+\sqrt{I}} - 0.3I\right] \quad (4)$$

where A is the Debye-Huckel limiting slope, having a numerical value of 0.51 at 25°C and 1 atmosphere pressure, and I is the ionic strength,[10,11,20] which is obtained through the expression

$$I = 0.5\,\Sigma\,[i]\,z_i^2 \quad (5)$$

The activity coefficient of uncharged molecules was estimated by[21]

$$\log f_0 = 0.5I \quad (6)$$

At pH extremes the stipulations of $I = 0.1$ and 0.005 used in these calculations may be exceeded because of the high concentrations of charged lead species, H^+ or OH^-. This is not considered to be an important problem for these purposes, however.

The total solubility was calculated by substitution of the appropriate cumulative formation constants (Table 2), ionic activities, and activity coefficients into the mass balance equation for lead [Eq (3)] giving

$$S_t = \frac{aPb^{2+}}{f_2} + \frac{\beta_{11}\,aPb^{2+}\,aOH^-}{f_1} + \frac{\beta_{11}\,aPb^{2+}\,aOH^-}{f_0} + \frac{\beta_{13}\,aPb^{2+}\,a^3OH^-}{f_1} + \frac{\beta_{21}\,a^2Pb^{2+}\,aOH^-}{f_3} + \frac{\beta_{34}\,a^3Pb^{2+}\,a^4OH^-}{f_2} + \frac{\beta_{44}\,a^4Pb^{2+}\,a^4OH^-}{f_4} + \frac{\beta_{68}\,a^6Pb^{2+}\,a^8OH^-}{f_4} + \frac{\beta_{c11}\,aPb^{2+}\,aCO_3^{2-}}{f_0} + \frac{\beta_{c12}\,aPb^{2+}\,a^2CO_3^{2-}}{f_2} \quad (7)$$

The activity of free lead ion is fixed by the solubility constants for each solid phase (Table 3), and these were solved for and substituted in place of aPb^{2+} in Eq (7).

The concentration of free carbonate ion in solution may be obtained from the ionization fraction expression[11,20]

$$[CO_3^{2-}] = \frac{C_t K_1' K_2'}{[H^+]^2 + [H^+]K_1' + K_1' K_2'} \quad (8)$$

where C_t is the total inorganic carbonate molarity, and K'_1 and K'_2 are the thermodynamic (infinite dilution) dissociation constants of carbonic acid (Table 3) corrected for ionic strength and temperature.

These calculations were performed by a FORTRAN IV-plus language program on the PDP 11/70 computer at the USEPA Environmental Research Center, Cincinnati, Ohio. A solubility curve was generated for each solid phase successively at a given C_t, and the final diagram was prepared by connecting the points of least solubility at each pH ($-\log aH^+$). Figures 1 and 2 are plots of the author's revised model [Eq (7)] showing the predicted lead concentration at various pHs at two ionic strengths and three total carbonate concentrations. An ionic strength of 0.005 is too low to permit a carbonate concentration of $10^{-1.1}$ M, so it is not shown. A series of curves was also prepared to show the effect on the dissolved lead concentration of CO_2 absorption from the atmosphere ($P_{CO_2} = 10^{-3.5}$ atm) in the high pH regions, if equilibrium levels of C_t were attained. Two such curves are shown in Figure 3.

To do this, the carbonate ion activity is related to atmospheric P_{CO_2} (the partial pressure of CO_2 gas) through the carbonic acid dissociation constants and the combined constant for CO_2 (g) hydration, K_H (Table 3). Solving these relations to put aCO_3^{2-} in terms of aH^+ and P_{CO_2} gives the relation

$$aCO_3^{2-} = \frac{K_H K_1 K_2 P_{CO_2}}{a^2H^+} \quad (9)$$

that was used in the program. For concentration units of moles per litre, P_{CO_2} is given in atmospheres.

To show the relationship between pH and C_t (total carbonate concentration) in another way, a different type of diagram was prepared by rearranging the program to calculate lead solubility as a function of total carbonate concentration at a series of fixed pH values and a given ionic strength. Several of these curves are shown in Figure 4.

Strictly speaking, in a true equilibrium "open system," degassing would take place when the initial amount of C_t added exceeded the theoretical level fixed by the atmospheric carbon dioxide content and the pH [Eq (9)]. This aspect was not incorporated into Figure 4, but is discussed elsewhere.[11]

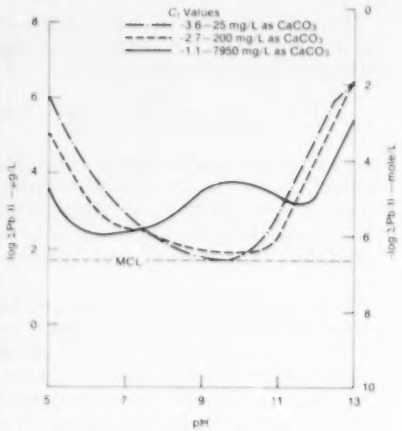

Figure 1. Revised model

I = 0.1; temperature = 25° C

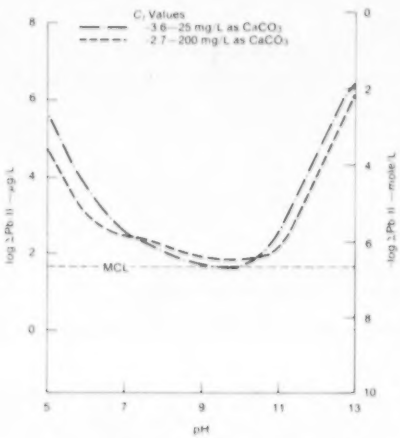

Figure 2. Revised model

I = 0.005; temperature = 25° C

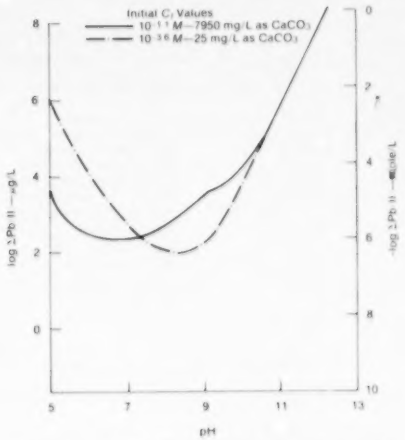

Figure 3. Revised model assuming CO_2 absorption from the atmosphere

$P_{CO_2} = 10^{-3.5}$ *atm; I = 0.1; temperature = 25° C*

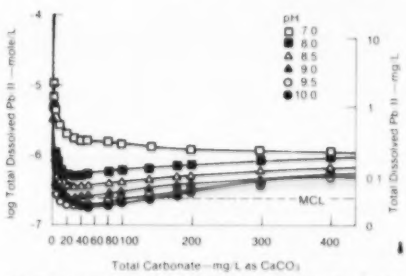

Figure 4. Plot of total dissolved Pb(II) vs C_t at fixed pH

I = 0.005; temperature = 25° C

Potential–pH relations. A tendency has existed among many who study corrosion processes to overlook the fact that the levels of metals in the solution, which is the primary concern when monitoring drinking water quality, are governed mainly by solubility considerations. This requires a detailed examination of all aqueous interactions that could govern the solubility of an element.

The solubility considerations are either kinetic (the relative rates of dissolution of the pipe material and precipitation of the solids of interest) or thermodynamic in nature. Little information exists on the reaction rates of the probable solids involved or on the adsorptive properties of scales commonly found on lead pipe or of the pipe itself. The focus here is on the evaluation of the solute species interactions behind the lead levels in a pure lead-water-carbonate system. This approach should yield much more accurate information as to the lead concentration limitations and passivation domains attainable than that provided by the consideration of only surface oxidation-reduction equations or by overly simplified ion-water-oxide discussions.

Three regions are normally differentiated in potential (E)-pH diagrams when applied to corrosion equilibria.[22] The area of immunity, sometimes called passivity, is the region in which the metal is not attacked. The area where the metal is protected by a coating of a sparingly soluble solid is that of passivation. The third is the region of active corrosion. The objective of corrosion control, then, is to adjust the solution composition, pH, and potential so that the amount of corrosion is minimized as much as is possible under any practical limitations imposed.

Caution must be observed when trying to quantitatively interpret such diagrams. In essence, they are a cross-section of a solubility diagram cut perpendicular to the plane of the concentration and pH axes, at a fixed metal concentration. Potential is established as the new axis, while pH is retained as the other. Obviously, they are limited to the choice of ionic strength, temperature, identity of species considered, and the concentrations stipulated. Less obvious is the limitation that when solubility equilibrium is maintained, the concentration of, in this case, Pb(II) varies with the pH as a result of its hydrolysis and carbonate complexation interactions. Adding new ligands or metals would further complicate the situation. Therefore, the specification of fixed total Pb(II) concentration, necessary to construct such a diagram in the first place, is only strictly correct in limited areas of the diagram. Additionally, in fields where an aqueous species predominates, no information is given as to the identity of the corroding surface phase.

The Gibbs free energy of formation data shown in Table 1 were used with a computer program written for an IBM WATFIV compiler[24] to calculate predicted E-pH stability fields. Figures 5 through 8 show these relations for two total dissolved lead concentrations (0.21 and 0.05 mg/L) and total dissolved carbonate concentrations (C_t) equivalent to 20 and 200 mg/L as $CaCO_3$. An ionic strength of zero is assumed, which will cause only a

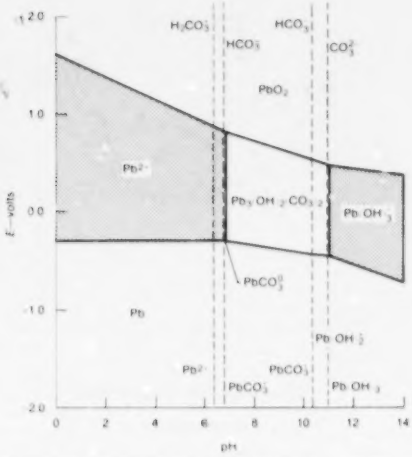

Figure 5. Potential–pH diagram for $C_t = 10^{-3.7}$ *M* (20 mg/L as $CaCO_3$) and dissolved Pb(II) species concentrations of 10^{-6} *M* (0.21 mg/L)

I = 0; temperature = 25° C; areas of passivation and immunity are unshaded.

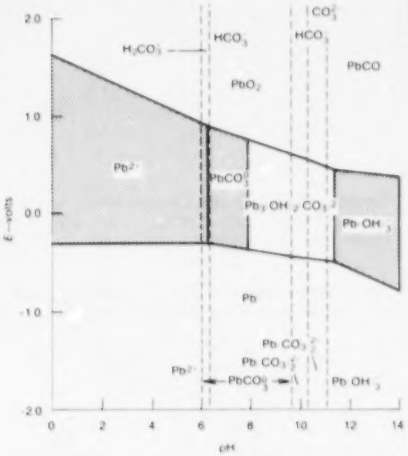

Figure 6. Potential–pH diagram for $C_t = 10^{-3.7}$ *M* (200 mg/L as $CaCO_3$) and dissolved species concentrations of $10^{-6.0}$ *M* (0.21 mg/L)

I = 0; temperature = 25° C; areas of passivation and immunity are unshaded.

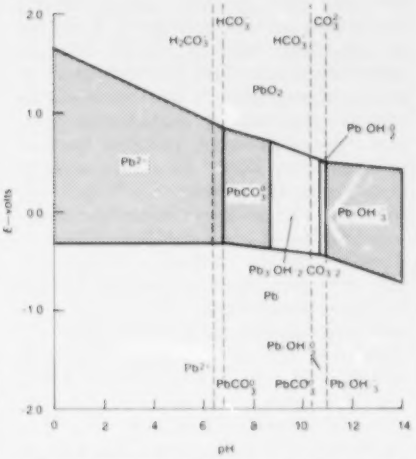

Figure 7. Potential–pH diagram for $C_t = 10^{-3.7}$ *M* (20 mg/L as $CaCO_3$) and dissolved Pb(II) species concentrations of $10^{-6.52}$ *M* (0.05 mg/L)

I = 0; temperature = 25° C; areas of passivation and immunity are unshaded.

small error because of the other uncertainties inherent in this type of diagram.

All of the species in Table 1 were considered, except CO_2 gas and $Pb(OH)_2$, aged. The decrease in the pH range of passivation (unshaded areas) because of the formation of lead carbonate complexes at increasing C_t is evident. This phenomenon was ignored in previously published potential–pH diagrams for the lead–carbonate–water system[6,22,23] and could lead to counterproductive treatment practices.

Experimentation

The author's revised model may be tested by comparison with several sets of experimental data. Patterson et al published results[6] of precipitation studies at known pH and total carbonate concentration (C_t), with analyses performed after a 4-hr reaction and 30-min settling time. Additionally, experiments have been and are being conducted by the EPA Drinking Water Research Division (DWRD) to simulate actual pipe conditions at fixed alkalinities of 10–20 mg/L, 50 mg/L, and 100 mg/L, all as $CaCO_3$, and at an input pH of 8.3–8.5. These data will be compared to the proposed new model for verification.

Briefly, in the DWRD study, water from a 1325-L (300-gal) fiberglass reservoir tank with floating lid was passed through a 31-m (100-ft) long pipe loop made from 2-cm (0.75-in.) inside diameter lead pipe. The water was passed daily during five cycles of varying durations (approximately 15–30 min) and flow rates of approximately 3.4–5.7 L/min (0.9–1.5 gpm) totaling 360–400 L (95–105 gal). The reservoir water was a mixture of Cincinnati, Ohio, tap water and deionized water from a strong acid–strong base mixed-bed exchanger. The desired pH was adjusted by addition of NaOH or HCl, and the alkalinity was adjusted by addition of $NaHCO_3$. A free chlorine residual of 0.1 to 0.6 mg/L as Cl was also maintained. Concentrations of Cl^- and SO_4^{2-} were also below $10^{-3.2}$ *M* (25 mg/L) and $10^{-3.77}$ *M* (16 mg/L), respectively, with total inorganic phosphate species ($[H_3PO_4^0] + [H_2PO_4^-] + [HPO_4^{2-}] + [PO_4^{3-}]$) below $10^{-5.7}$ *M* (0.2 mg/L as PO_4^{3-}). Between the 50 mg/L as $CaCO_3$ alkalinity and 100 mg/L as $CaCO_3$ alkalinity runs, the pipe was cleaned by a 4-hr flush with 1 percent acetic acid, followed by a quick rinse with deionized water and immediate filling with water at 100 mg/L alkalinity as $CaCO_3$.

After the water completed its passage through the 31-m (100-ft) lead pipe loop, it was sent through plastic pipe and tubing to a 380-L (100-gal) plastic holding tank. This tank fed a small recirculation loop with several sections of identical 2-cm (0.75-in.) lead pipe upon which corrosion rate measurements were made by a linear polarization technique.[25] During the inital 10–20 mg/L as $CaCO_3$ alkalinity experiment, the tank had a fixed lid which allowed absorption of atmospheric CO_2 gas, lowering the pH. For subsequent runs the tank was fitted with a floating PVC lid that allowed the pH to be maintained very close to 8.5.

Samples were taken after various lengths of standing time (by activating a 0.09-L/s [1.5-gpm] pump) and during the pumping immediately following the standing sample. The samples were

drawn through a PVC plastic tap with polyethylene tubing located at the end of the 31-m (100-ft) pipe loop.

Initially, these samples were analyzed for total lead (graphite furnace atomic absorption spectrophotometry[26]), pH, total alkalinity, calcium (EDTA titration with Solochrome dark blue indicator[27] or atomic absorption[27,28]), and free available chlorine (test 409C[27]). Periodically, samples were additionally analyzed for total hardness (test 309B[27] or atomic absorption[27]), specific conductance,[28] and temperature. The reservoir water was monitored for the above parameters plus total dissolved solids, sodium, chloride, sulfate, orthophosphate, potassium, and silica on a routine basis. All samples for lead and samples not to be analyzed the same day for other metals were preserved with 1.5 mL concentrated HNO_3 per litre sample volume; samples for orthophosphate and nitrate were preserved with 1.5 mL $HgCl_2$ per litre sample volume. After the observation that any change in calcium concentration between the reservoir water and the standing samples was less than the analytical precision of the method, the calcium test was put on a periodic monitoring basis.

Sample pH measurements were done after two-point standardization with slope compensation using a combination electrode with thallium amalgam internals mounted in a stopper and a digital pH meter reading to three decimal places. The samples for this measurement were taken in 50-mL Erlenmeyer flasks sealed with plastic or rubber stoppers immediately after filling (allowing no air space). The electrode assembly was immersed in each sample following the addition of a stirring bar, providing a seal against atmospheric CO_2 exchange and vastly improved pH precision and accuracy for poorly buffered waters. Duplicate samples were taken, the first for equilibration and the second for the recorded reading.

Total alkalinity values were determined for routine monitoring purposes by titration with 0.020 *N* HCl to endpoint pH values of 5.3 (10 to 20 mg/L as $CaCO_3$ total alkalinity), 5.1 (50 mg/L as $CaCO_3$ alkalinity), and 4.85 (100 mg/L as $CaCO_3$ alkalinity). These pH values were observed to be sufficiently close approximations to the $H_2CO_3^* - HCO_3^-$ equivalence point ($H_2CO_3^* = CO_2$ aq + $H_2CO_3^0$ after the convention of Stumm and Morgan[11]) determined by potentiometric titration curves for this study. Endpoints were obtained using either a digital pH meter or a neutralized mixed bromocresol green–methyl red indicator with molar ratios varied to give the desired transition point. Titrations were carried out with slow stirring in closed Erlenmeyer flasks or 200-mL beakers. Comparisons with EPA quality-control standards indicated better than ± 2 percent relative accuracy with even the lowest alkalinity samples.

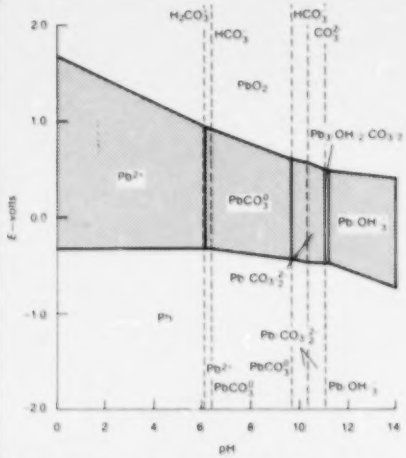

Figure 8. Potential–pH diagram for $C_t = 10^{-2.7}$ *M* (200 mg/L as $CaCO_3$) and dissolved Pb(II) species concentrations of $10^{-5.92}$ *M* (0.05 mg/L)

I = 0; temperature = 25° C; areas of passivation and immunity are unshaded.

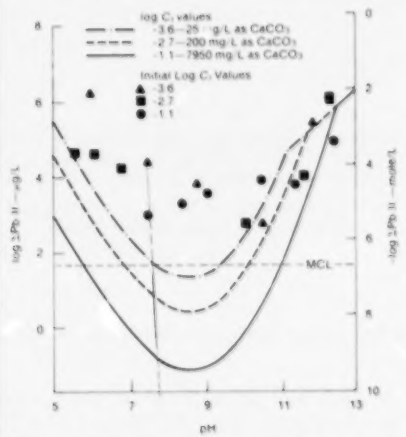

Figure 9. Recreation of the model of Patterson et al[9]

I = 0; temperature = 25° C

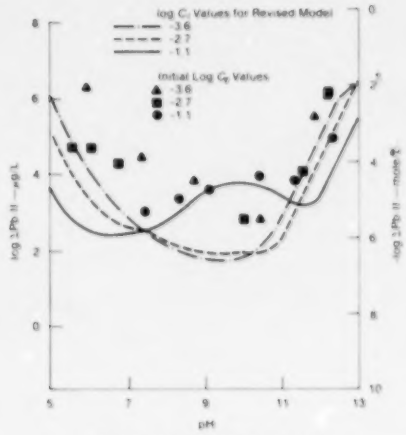

Figure 10. Revised model

I = 0.1; temperature = 25° C

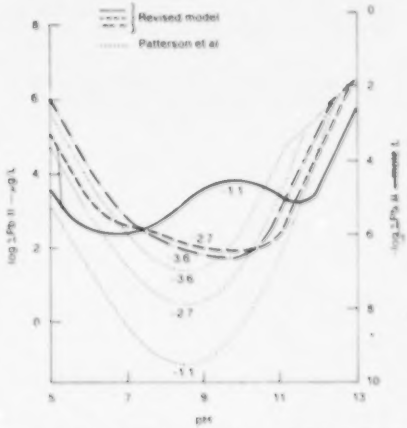

Figure 11. Direct comparison of the revised solubility model with two solid phase model without carbonate complexation of Patterson et al[9]

Values given are log C_t—mole/L

Because of the low relative concentrations of other acid-neutralizing species, the total alkalinity titrations are directly relatable to C_t by[11,29]

$$Alk_t = [HCO_3^-] + 2[CO_3^{2-}] + [OH^-] - [H^+] \quad (10)$$

wherein Alk_t is expressed as equivalents/litre for molar concentrations of the other species. The ionization fraction expressions[11,29,29] may be substituted for the first two terms, and this upon rearranging Eq (10) gives

$$C_t = (Alk_t + [H^+] - [OH^-]) \frac{[H^+]^2 + K_1'[H^+] + K_1'K_2'}{[H^+]K_1' + 2K_1'K_2'} \quad (11)$$

For the dilute ionic strengths and particular pH values employed, C_t values calculated in test cases by Eq (11) and by a more rigorous computer algorithm[30] agree with those obtained directly by the previously outlined titration procedure within 5 percent, a close percentage when analytical and calculation uncertainties are considered. Therefore, most reported C_t values were converted directly from titration data.

No interference from $CaCO_3$ precipitation in the pipe loop is considered likely. The saturation index[30,31] (SI) for any solid may be defined as

$$SI = \log \frac{\text{ion activity product}}{K_{so}} \quad (12)$$

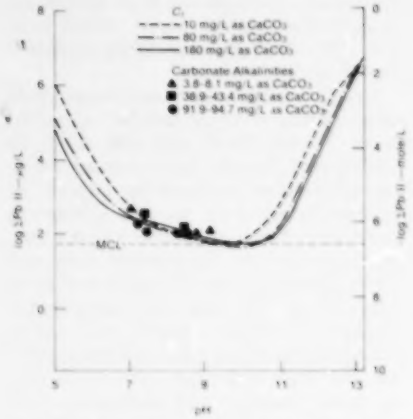

Figure 12. Coupon test data compared with revised model

I = 0.005; temperature = 25° C

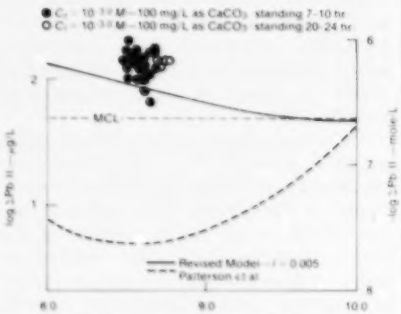

Figure 14. Comparison of lead pipe solubility data with two models

Test duration—89 days.

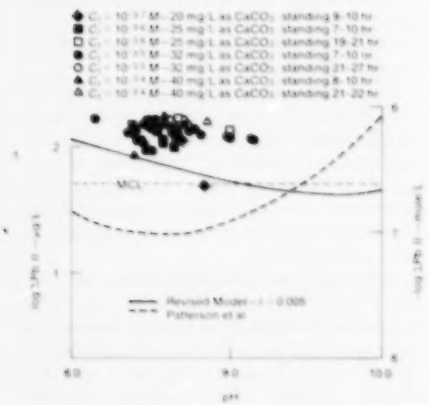

Figure 13. Comparison of lead pipe solubility data with two models

Test duration—94 days.

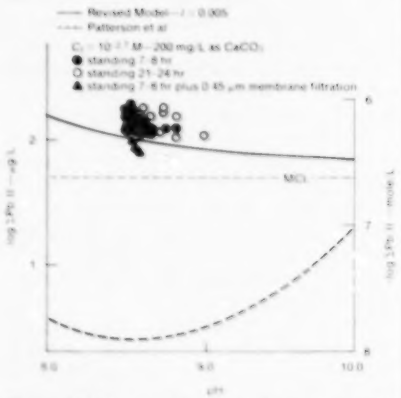

Figure 15. Comparison of lead pipe solubility data with two models

Temperature—25°C; test duration—more than 240 days.

which for $CaCO_3$ is

$$SI = \log \frac{aCa^{2+} \cdot aCO_3^{2-}}{K_{so}} \qquad (13)$$

Positive values of SI indicate oversaturation, while negative values indicate undersaturation. The size of SI is a direct reflection of the magnitude of the state.

Saturation indexes were obtained using a version of the WATSPEC equilibrium aqueous speciation program expanded by this author and run on an IBM 370/168 computer. This program corrects for temperature, ionic strength, major complexes, and ion pairs. K_{so} values were considered for calcite,[32,33] argonite,[30,33] and a fresh precipitate.[34] The low concentrations of calcium, generally 3-6 mg/L as Ca, gave SI values of –0.1 or less for calcite, the least soluble $CaCO_3$ phase, in almost all cases.

Results and discussion

Comparison of models. The orginal model presented by Patterson et al[6] and utilized by O'Brien,[7] as recreated by the lead solubility computer program, is shown in Figure 9. All constants were taken directly from the original or were derived from information contained within, and no corrections were made for ionic strength or carbonate complexation. Also shown are the Patterson et al precipitation data[6] from the cited laboratory experiments, giving the initial values of C_t (defined as $[H_2CO_3^*] + [HCO_3^-] + [CO_3^{2-}]$ when other carbonate complexes are insignificant) and the final concentrations of lead. This shows that the Patterson et al model does not agree well with the experimental data.[6]

Verification of revised model—precipitation data. Figure 10 is the revised model representing the solution of Eq (7) at an ionic strength of 0.1 and 25° C, along with the same precipitation data, and shows the better agreement obtained with the revised model. The curve morphology is greatly complicated, and the predicted equilibrium Pb(II) solubility would be expected to increase by several orders of magnitude over that suggested by Patterson et al,[6] Hem and Durum,[5] and O'Brien[7] (Fig-ure 11).

Furthermore, the trends in solubility with C_t completely reverse themselves twice, at pH values of approximately 7.3 and 11.8. In the pH range of 7 to 10 (probably the range of most interest to the water treatment industry) the relationship between lead solubility and total carbonate concentration is exactly the opposite of that predicted by three of the previous models.[5-7] Finally, the predicted equilibrium lead concentrations using this model are also seen to be above the MCL of 0.05 mg/L in all pH regions in systems of moderate to high C_t (approximately 140 mg/L as $CaCO_3$ and higher) and very low carbonate content (less than approximately 10 mg/L as $CaCO_3$). Separate consideration of the model omitting the polymeric lead hydroxide species revealed that they could be neglected without noticeable effect in the pH range studied.

In comparison to the Patterson et al precipitation data,[6] the original two solid phase models greatly underestimate the solubility of Pb(II) at all values of C_t, except at pH extremes (Figure 9). This deviation was attributed by Patterson et al[6] to incomplete solids separation, insufficient reaction time, and the possible lack of applicability of published solubility product constant data to the age and purity of the precipitates experimentally obtained. Further, the existence of metastable polymorphs with slow conversion times and widely differing solubilities has been pointed out for $Zn(OH)_2$ (s),[35] for example. In addition, a given solid may contain lattice defects, and any change in particle size of specific surface may change its Gibbs free energy[15] and consequently its solubility constant. Finally, slow precipitation rates for metal carbonates from low-C_t systems have also been observed.[33]

Although these are quite plausible explanations for some of the deviations, they seem to fall short in explaining both the magnitude of the discrepancy, especially in the $C_t = 10^{-1.1}$ M system where the most complete reaction would be expected and the observed deviation is the highest, and the lack of similarity

between the predicted and observed curve shape at pHs below approximately 12 [$Pb(OH)_2(s)$ field]. Addition of $Pb_3(OH)_2(CO_3)_2(s)$ alone to the two solid phase model would still predict solubilities far below those observed during the precipitation studies.

The author's revised model (Figure 10) shows excellent agreement with the precipitation data at log $C_t = -1.1$ M. Although the data do not fit as well to the other appropriate curves, their trends generally agree better with those curves (especially with respect to pH of minimum solubility) than does the simple two solid phase model[6] (Figure 9).

Influence of carbon dioxide. Some of the other deviations shown in Figure 10 may be explained by Figure 3, where equilibrium with atmospheric carbon dioxide at high pH ($P_{CO_2} \sim 10^{-3.5}$ atm) is assumed. The specification of fixed C_t for cases that are actually an open system[10,11,29] is only rigorously valid when C_t from added carbonate salt is much greater than that obtained from the atmosphere directly and no degassing occurs. For $C_t = 10^{-3.6}$ M this would be around pH 7; for $C_t = 10^{-1.1}$ M, around pH 9. The hydration reaction

$$CO_2\,(g) + H_2O \rightarrow H_2CO_3^* \qquad (14)$$

is not very fast.[11] However, the linearity of experimental precipitation data[6] (Figure 10) above approximately pH 11 regardless of specified C_t is an indication of the operation of this control mechanism, even though actual equilibrium with the atmosphere was not attained. Actual C_t values analyzed by Patterson et al[6] reinforce this explanation.

Static coupon tests. Patterson and O'Brien published a series of coupon tests of nine and thirty days duration at known C_t and pH under static conditions.[6] The coupons were left to corrode freely in water with four initial C_t levels and at starting pH values of 7 and 8. The published data points are plotted in Figure 12 along with curves from the author's model at similar C_t values. The agreement of the data and model is very good. The model also correctly predicts that high C_t levels ($\simeq$ 180 mg/L as $CaCO_3$) would provide better protection at a pH of approximately 7, but not at the higher pH values tested.

Verification of revised model—pipe loop data. The pipe loop experimental data, like the coupon tests, represent a more truly closed system than that of the precipitation studies and initially approaches solubility equilibrium from the opposite direction. Figures 13 through 15 show data from three different experiments, each of several months' duration, compared to the appropriate curve generated by Eq (7) for $I = 0.005$ and the equivalent curve of the two solid phase model depicted in Figure 9.[6,7] In Figures 13–15, data from overnight equivalent standing are differentiated from those of a longer duration. Very good to excellent agreement is obtained in all cases with the predictions of the author's solubility model over this carbonate concentration range, but not with the previous two solid phase models that ignored lead carbonate complexes. The undersaturation predicted at low C_t (Figure 13) seems to lessen as C_t increases (Figures 14, 15).

This probably is not caused by weak sulfate,[14] chloride,[14,37] or phosphate complexation,[38] as these ligands were maintained at low levels. The underestimation could be the result of some of the kinetic and thermodynamic considerations[35,36] discussed previously, as a state of saturation or supersaturation must be attained first for carbonate, hydroxide, or hydroxycarbonate precipitation to be the operating concentration control mechanism. This suggestion is supported by the observation that the low-C_t experiments of all three methods—precipitation, coupons, and pipe loop data—tend to give slightly higher solubilities in practice than the thermodynamic model would predict, while those at the higher carbonate concentrations closely conform to the theoretical predictions.

In the pipe loop experiment, however, a major cause may also be that the velocity or turbulence (or both) of the water flow during sampling for the standing samples is sufficient to dislodge weakly adhering fresh precipitate. In an attempt to evaluate this, several overnight standing samples in the $C_t = 200$ mg/L as $CaCO_3$ run were split, with one part filtered through 0.45-μm cellulose acetate membranes before acidification. These data are also plotted in Figure 15. Because some lead was lost during filtration of acidified lead standards (10 to 20 percent), the actual concentration of dissolved lead in solution would lie between the filtered and unfiltered values. Lead losses during filtration of similar amounts have been reported previously.[39] Therefore, precipitate or corrosion product was probably dislodged by the water flow. Similar data are not available for the lower C_t runs.

No measurements of the redox potential of the solutions were performed in this study. Assuming the potentials were near or within the hypothetical stability boundaries of water (between approximately −0.5 V and +0.7 V at pH 8.5),[10,11] the predictions of Figures 5 through 8 are also confirmed, with passivation not established until the dissolved lead concentration considerably exceeded 0.05 mg/L.

In contrast to the overnight standing samples (Figures 13–15), all three concentrations of carbonate employed in the pipe loop study are seen to generally reduce the total lead level in flowing samples to below the MCL (Figure 16). The range is approximately 0.02 to 0.04 mg/L for most samples. The high carbonate system (200 mg/L as $CaCO_3$) is seen to marginally increase the lead concentrations in the running water, which is in line with the higher solubility predicted by the author's model.

Linear polarization corrosion rate measurements[25] show similar corrosion rates for the 20–40 and 100 mg/L as $CaCO_3$ runs, but the high carbonate system showed an increase by a factor of approximately two to ten. Observed rates were approximately 0.1 to 0.2 mils per year (mpy) for the first two runs, and 0.5 to 2.0 mpy for the 200 mg/L as $CaCO_3$ experiment. The first two experiments attained a fairly stable level after decreasing during a short induction period. The high carbonate system showed an initial increase and continuing drift even after more than nine months of constant water circulation. Two different sets of electrodes show the same behavior, further corroborating the solubility data. Also, in the pH range studied (8.3 to 8.5), neither of the higher carbonate systems appear to lead to a more adherent film than at the lower dosage, since more sloughing off of film or corrosion product was observed than in the 20 to 40 mg/L as $CaCO_3$ run.

Influence of standing time. No systematic program of sampling to determine rates of lead uptake by the standing water was undertaken. Table 4, however, shows some data taken after comparatively short periods of standing time, indicating the rapid increase in the lead concentration in the pipe.

Uncertainty of equilibrium constants. The predicted Pb(II) solubility of this and any other thermodynamic model has some minimum quantitative uncertainty associated with it, stemming from several factors. A range of β values for hydroxide and carbonate complexes of lead exists in the literature, and these are not mutually independent. Thus, the overall effect is difficult to evaluate exactly. For instance, the use of β_{11}, β_{12}, and β_{13} from the Baes and Mesmer critical compilation[10] with the same β_{c11} and β_{c12} given in Table 3 gives a slightly lower predicted lead solubility. Higher β_{c11} and β_{c12} values[14] lead to a higher solubility prediction in the pH range of approximately 6 to 10 (depending on C_t). Additionally, uncertainty exists in the published K_{sp} values for $Pb_3(OH)_2(CO_3)_2(s)$ and $PbCO_3(s)$ because carbonate complexation of the dissolved lead may not have been properly taken into account during the experimental data reduction, or an inconsistency may exist between the values of the formation constants of lead hydroxide complexes used by the original experimenter and those used in the solubility model. At present, however, compelling evidence is not thought to exist for the use of alternative constants available,

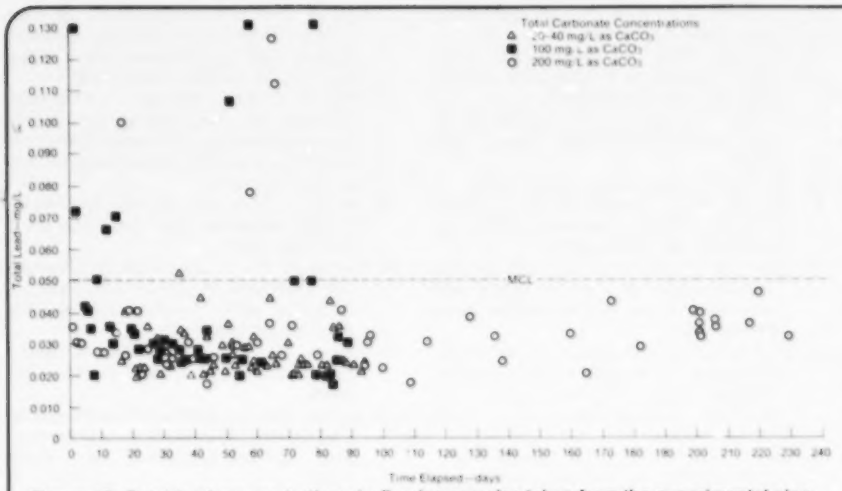

Figure 16. Total lead concentrations in flowing samples taken from the experimental pipe loop

TABLE 4
Increase in lead concentration during short standing periods

Alk_t mg/L as $CaCO_3$	Hours Standing	Initial pH	Initial Total Pb*	Final pH	Final Total Pb	Next Flow Total Pb
16.0	1.5	8.30	0.030	†	0.082	0.026
16.0	1.5	8.50	0.032	†	0.078	0.024
16.0	1.9	8.30	0.029	8.36	0.125	†
16.2	3.	8.35	†	8.42	0.082	0.036
18.5	1.5	8.36	†	8.40	0.084	0.032
47.2	1.5	8.44	†	8.45	0.110	0.020
51.3	1.3	8.57	†	8.58	0.100	0.035
101	1.9	8.52	0.043	†	0.090	†
102	1.8	8.52	†	†	0.104	†
103	1.9	8.66	†	8.66	0.092	†
100	1.6	8.50	0.036	8.51	0.125	0.035

* = Value given is for the flowing sample immediately preceding; input water from the reservoir tank was less than 0.005 mg/L in lead for all cases.
† = not analyzed

when the other kinetic, thermodynamic and analytical uncertainties involved in these models are considered.

Summary

The direct application of the author's revised model [primarily Eq (7)] to quantitatively and accurately predict concentrations of lead in tap water may not be possible in many instances. This is in no way a fault of the model itself. In any distribution system, many chemical and physical concentration control mechanisms are operating simultaneously. First, the relative importance of the lead carbonate and hydroxycarbonate solubility-complexation equilibria is not necessarily constant from system to system, or even from one part of a system to another. Second, the nature and thickness of existing scale layers could be the dominant control, as well as such factors as the redox potential of the water, saturation state with respect to other solids (for example, lead orthophosphates[41,42] or $CaCO_3$), sorption equilibria of both lead[14] and possible ligands (organic[43] and inorganic), temperature, and dissolved oxygen. Finally, the system under consideration may not have even attained equilibrium.

The model is quite useful, however, because of the good correlation with near-equilibrium experimental data. This model, then, may be employed with some confidence in determining whether or not, in fact, a given lead level could be controlled by a simple solubility mechanism, whether insufficient information exists, or whether another explanation need be sought. Using the earlier models without consideration of hydrocerussite and lead carbonate complexes, the lack of agreement with experimental results left considerable room for error in prediction of lead solubility.

For areas experiencing high lead values in the tap water, this model suggests a somewhat different alkalinity and pH combination than has been stated previously[6-9,22,23] for carbonate water treatment and gives less optimistic estimates of the potential reduction attainable, although reduction below the MCL of 0.05 mg/L could still be possible.

Figure 4 and the experimental data (Figures 13-16) thus far show little advantage in continuing to increase the carbonate level beyond approximately 30-40 mg/L as $CaCO_3$ in the pH range of 8 to 9.5. A minimum concentration of carbonate is necessary to overcome the higher solubility of $Pb(OH)_2(s)$, but a continual increase in carbonate concentration will promote the formation of the complexes $PbCO_3^0$ and $Pb(CO_3)_2^{-2}$, thus actually increasing the molar solubility of lead. None of the three types of tests conducted—precipitation, coupon, or pipe loop—resulted in the reduction of the total lead level in the solution for standing samples to below the 0.05-mg/L MCL at total carbonate concentrations of 0 to 7950 mg/L as $CaCO_3$. Dosages of approximately 30 to 200 mg/L as $CaCO_3$ in the pH range of 8 to 9 did, however, result in considerable reduction of total lead content over what it would have been in systems containing no or very little carbonate.

Practical considerations in developing a treatment methodology for lead pipe should include the assurance of an adequate buffer capacity of the water[13,17] so that the OH^- produced in the corrosion process will not shift the pH high enough to increase the overall lead solubility by formation of lead hydroxide complexes (where the curves in Figures 1 and 2 bend upwards at high pH). Local points of high pH may also serve to make any precipitated scale more permeable. Carbonate treatment levels of 30 to 60 mg/L probably provide quite adequate buffer capacity for most water compositions and standing times.

Field data[1,13] indicate that total lead levels may be reduced farther below the MCL than predicted by the model presented here or by the cited laboratory experiments. This is probably related to the surface properties of the pipe, or possibly other precipitation equilibria in the solution. These aspects need further research to determine their actual role, so that pH and carbonate adjustment can be optimized to take advantage of these factors.

The pipe loop data presented here do not differentiate between the total lead carried by the water and that in true aqueous solution for the lower two carbonate concentrations tested. The ability of a film at a given C_t and pH to consistently adhere to the surface of the pipe is also a practical consideration of great significance. The best combination of C_t and pH may have to be experimentally determined in each case, until further research sheds light on the scale properties as these two parameters are varied.

Future work

The role the aforementioned factors play in dictating the observed lead solubility needs to be further examined by careful correlation of field observations with laboratory experimentation and modeling, so that efficient predictions of optimum treatment methodologies can be made in terms of time, cost, and absence of deleterious side effects. Field data must include physical examination of pipes or pipe samples plus a comprehensive chemical characterization of the water at the plant outflow and, most importantly, at the consumer's tap. An analysis of surficial composition would

also be useful. Techniques such as Raman and infrared spectroscopy" may prove helpful in that regard. Determination of pH, alkalinity for total carbonate concentration calculation, and temperature should be done on location, or immediately upon return with proper precautions. This is especially important in the case of poorly buffered waters. Filtration of the samples before addition of any preservative would enable some differentiation between soluble and suspended components, possibly also important for health effects studies. Laboratory analysis should include major cations and anions, as well as such ligands as sulfate, inorganic phosphate, chloride, fluoride, and silica. Measurements of parameters that may be related to the redox potential of the solution would also be desirable. Much of the data already collected is not useful because of the absence of analyses of major solubility-controlling factors.

Acknowledgments

The author gratefully acknowledges the assistance of Marvin Gardels, res. chemist, and Ralph Buelow, res. sanitary engr., both of the physical and chemical contaminants removal branch, Drinking Water Research Division, US Environmental Protection Agency, who were primarily responsible for the design and construction of the laboratory solubility experiment. Also, credit is due William Mueller for suggestions concerning pH measurement, Leown Moore and James M. Symons for manuscript criticism, and members of the analytical support group, Drinking Water Research Division, who performed many of the analyses.

References

1. Zoetman, B.C.J. & Haring, B.J.A. Introduction of Chemical Compounds into Drinking Water During Distribution. R.I.D.–Medeling 78-6. *Rijksinstituut voor Drinkwatervoorziening*, The Netherlands (1978).
2. Karalekas, P.C. et al. Lead and Other Trace Metals in Drinking Water in the Boston Metropolitan Area. Proc. AWWA 95th Ann. Conf., Minneapolis, Minn. (1975).
3. Karalekas, P.C. et al. Alternative Methods for Controlling the Corrosion of Lead Pipe. *Jour. NEWWA*, 92:159 (1978).
4. National Interim Primary Drinking Water Regulations. EPA-570/9-76-003. Ofce. of Wtr. Sply., Washington, D.C. (1976).
5. Hem, J.D. & Durum, W.H. Solubility and Occurrence of Lead in Surface Water. *Jour. AWWA*, 65:8:562 (Aug. 1973).
6. Patterson, J.W. et al. Carbonate Precipitation for Heavy Metals Pollutants. *Jour. WPCF*, 49:2397 (1977)
7. O'Brien, J.E. Lead in Boston Water: Its Cause and Prevention. *Jour. NEWWA*, 90:173 (1976).
8. Patterson, J.W. & O'Brien J. Control of Lead Corrosion. *Jour. AWWA*, 71:5:284 (May 1979).
9. Wagman, D.D. et al. US Natl. Bur. Stand. Tech. Note 270-3 (1968).
10. Garrels, R.N. & Christ, C.L. *Solutions–Mineral and Equilibria*. Harper and Row, New York (1965).
11. Stumm, W. & Morgan, J.J. *Aquatic Chemistry*. Wiley-Interscience, New York (1970).
12. Personal communication (May, 1979).
13. Schock, M.R. Drinking Water Research Division, USEPA, Cincinnati, Ohio, unpublished data (1978–1979).
14. Hem, J.D. Geochemical Controls on Lead Concentrations in Stream Water and Sediments. *Geochim. Cosmochim. Acta*, 40:599 (1976).
15. Zirino, A. & Yammamoto, S. A pH-Dependent Model for the Chemical Speciation of Copper, Zinc, Cadmium, and Lead in Seawater. *Limnol. Oceanogr.*, 17:661 (1972).
16. Long, D.T. & Angino, E.E. Chemical Speciation of Cd, Cu, Pb, and Zn in Mixed Freshwater, Seawater, and Brine Solutions. *Geochim. Cosmochim. Acta*, 41:1183 (1977).
17. Vuceta, J. & Morgan, J.J. Chemical Modeling of Trace Metals in Fresh Waters: Role of Complexation and Adsorption. *Environ. Sci. Technol.*, 12:1302 (1978).
18. Sibley, T.H. & Morgan, J.J. Equilibrium Speciation of Trace Metals in Freshwater:Seawater Mixtures. Symp. Proc. Intern. Conf. on Heavy Metals in the Envir., Toronto, Canada (Oct. 27, 1975).
19. Bilinski, H. et al. Determination of the Stability Constants of Some Hydroxo and Carborato Complexes of Pb(II), Cu(II), and Zn(II) in Dilute Solutions by Anodic Stripping Voltammetry and Differential Pulse Polarography. *Anal. Chim. Acta*, 84:157 (1976).
20. Butler, J.N. *Ionic Equilibrium: A Mathematical Approach*. Addison-Wesley, Palo Alto, Calif. (1964).
21. Reardon, E.J. & Langmuir, D. Activity Coefficients of $MgCO_3^0$ and $CaSO_4^0$ Ion Pairs as a Function of Ionic Strength. *Geochim. Cosmochim. Acta*, 40:549 (1976).
22. Delahay, P. et al. Potential-pH Diagram of Lead and Its Applications to the Study of Lead Corrosion and to the Lead Storage Battery. *Jour. Electrochem. Soc.*, 98:57 (1951).
23. Pourbaix, M. *Atlas of Electrochemical Equilibria in Aqueous Solutions*. Pergammon Press, Oxford; cebelcor, Brussels (1966).
24. Froning, M.H. et al. An Improved Method for Calculation of Potential-pH Diagram of Metal-Ion-Water Systems by Computer. *Corrosion Sci.*, 16:371 (1976).
25. Gardels, M.C. Drinking Water Res. Div., USEPA, Cincinnati, Ohio, unpublished data (1978-1979).
26. Methods for Chemical Analysis of Waters and Wastes. EPA-600/4-79-020, Environmental Monitoring and Support Laboratory, USEPA (1979).
27. *Standard Methods for Examination of Water and Wastewater*. APHA, AWWA, and WPCF, Washington, D.C. (14th ed., 1976).
28. Brown, E. et al. Methods for the Collection and Analysis of Water Samples for Dissolved Minerals and Gases. *USGS Techniques for Water Resource Investigation*, (1970).
29. Loewenthal, R.E. & Marais, G.V.R. *Carbonate Chemistry of Aquatic Systems: Theory and Applications*. Ann Arbor Science, Ann Arbor, Mich. (1976).
30. Wigley, T.M.L. watspec: A Computer Program for Determining the Equilibrium Speciation of Aqueous Solutions. British Geomorphol. Res. Group Technical Bull. 20 (1977).
31. Wigley, T.M.L. Ion Pairing and Water Quality Measurements. *Can. Jour. Earth Sci.*, 8:468 (1971).
32. Jacobson, R.L. & Langmuir, D. Dissociation Constants of Calcite and $CaHCO_3^+$ from 0 to 50°C. *Geochim. Cosmochim. Acta*, 38:301 (1974).
33. Christ, C.L. et al. Stabilities of Calcite and Argonite. *Jour. Res. USGS*, 2:175 (1974).
34. Suarez, D.L. Ion Activity Products of Calcium Carbonate in Water Below the Root Zone. *Soil Sci. Soc. Amer. Jour.*, 41:310 (1977).
35. Schindler, P.W. Heterogeneous Equilibria Involving Oxides, Hydroxides, Carbonates, and Hydroxide Carbonates. *Equilibrium Concepts in Natural Water Systems*, Advances in Chemistry Series 67 (Robert F. Gould, editor). Amer. Chem. Soc., Washington, D.C. (1976).
36. Hem, J.D. Chemistry and Occurrence of Cadmium and Zinc in Surface and Groundwater. *Water Res.*, 8:661 (1972).
37. Hahne, H.C.H. & Kroontje, W. Significance of pH and Chloride Concentration on Behavior of Heavy Metal Pollutants: Mercury(II), Cadmium(II), Zinc(II), and Lead(II). *Jour. Environ. Quality*, 2:444 (1973).
38. Nriagu, J.O. Lead Orthophosphates, I. Solubility and Hydrolysis of Secondary Lead Orthophosphate. *Inorg. Chem.*, 11:2499 (1972).
39. Das, H.A. & van der Sloot, H.A. Sampling Problems and the Determination of Mercury in Surface Water, Seawater, and Air. *Natl. Bur. of Standards Special Publ.* 422 (Phillip D. LaFleur, editor). US Gov. Printing Ofce., Washington, D.C. (1976).
40. Baes, C.F. & Mesmer, R. *The Hydrolysis of Cations*. John Wiley and Sons, New York (1976).
41. Nriagu, J.O. Lead Orthophosphates, II. Stability of Chloropyromorphite at 25°C. *Geochim. Cosmochim. Acta*, 37:367 (1973).
42. Nriagu, J.O. Lead Orthophosphates, IV. Formation and Stability in the Environment. *Geochim. Cosmochim. Acta*, 38:887 (1974).
43. Healy, T.W. Principles of Adsorption of Organics at Solid-Solution Interfaces. *Jour. Macromol. Sci-Chem.*, A8:603 (1974).
44. Thibeau, R.J. et al. Infrared and Raman Spectroscopy of Aqueous Corrosion Films on Lead. *Jour. Electrochem. Soc.*, 127:27 (1980).

A paper contributed to and selected by the JOURNAL, authored by Michael R. Schock (Active Member, AWWA), chemist, drinking water res. div., USEPA, Cincinnati, Ohio.

76094 3510, 4300

If you buy sodium Hypochlorite for safe, effective water treatment...

compare KUEHNE to your present supplier and you'll take the KUEHNE alternative!

Kuehne Chemical	Your present supplier
☑ 24-hour, 7 day delivery service (Kuehne's never closed, you get deliveries when you need them)	☐
☑ Kuehne produces its own chemicals (we don't repackage products made by others so we control quality and availability)	☐
☑ Deliveries you can depend upon (Kuehne has never failed to deliver due to allocations or weather)	☐
☑ Kuehne's Pledge of Quality (We produce from virgin stock with consistent strength and stability from batch to batch)	☐
☑ Free Consulting Service (A Kuehne exclusive. Customers may receive our help with personnel training problems, EPA and OSHA regulations, storage and movement systems, etc.)	☐

A REGIONAL, DEPENDABLE SOURCE FOR THESE BASIC CHEMICALS:

SODIUM HYPOCHLORITE

LIQUID CHLORINE

CAUSTIC SODA

MURIATIC ACID

Specialists in Tank Truck Deliveries!

KUEHNE CHEMICAL COMPANY

(201) 862-1212

14 COMMERCE DRIVE, CRANFORD, N.J. 07016

Reader Inquiry Service No. 023

Erratum

Several errors appeared in the "Response of Lead Solubility to Dissolved Carbonate in Drinking Water" (SCHOCK, M.R. *Jour. AWWA*, 72:12:695 [Dec. 1980]). The correct information is printed below.

TABLE 2

Calculated formation constants of complexes of Pb(II) at 25°C

Reaction	Name of Constant	Log β
$Pb^{2+} + OH^- \rightleftharpoons PbOH^+$	β_{11}	6.77
$Pb^{2+} + 2OH^- \rightleftharpoons Pb(OH)_2^0$	β_{12}	11.67
$Pb^{2+} + 3OH^- \rightleftharpoons Pb(OH)_3^-$	β_{13}	13.90
$2Pb^{2+} + OH^- \rightleftharpoons Pb_2OH^{3+}$	β_{21}	7.63
$3Pb^{2+} + 4OH^- \rightleftharpoons Pb_3(OH)_4^{2+}$	β_{34}	32.10
$4Pb^{2+} + 4OH^- \rightleftharpoons Pb_4(OH)_4^{4+}$	β_{44}	35.08
$6Pb^{2+} + 8OH^- \rightleftharpoons Pb_6(OH)_8^{4+}$	β_{68}	68.31
$Pb^{2+} + CO_3^{2-} \rightleftharpoons PbCO_3^0$	β_{c11}	7.10
$Pb^{2+} + 2CO_3^{2-} \rightleftharpoons Pb(CO_3)_2^{2-}$	β_{c12}	10.33

$$S_t = \frac{\alpha Pb^{2+}}{f_2} + \frac{\beta_{11}\,\alpha Pb^{2+}\,\alpha OH^-}{f_1} + \frac{\beta_{11}\,\alpha Pb^{2+}\,\alpha OH^-}{f_0} + \frac{\beta_{13}\,\alpha Pb^{2+}\,\alpha^3 OH^-}{f_1} + \frac{\beta_{21}\,\alpha^2 Pb^{2+}\,\alpha OH^-}{f_3} + \frac{\beta_{34}\,\alpha^3 Pb^{2+}\,\alpha^4 OH^-}{f_2} + \frac{\beta_{44}\,\alpha^4 Pb^{2+}\,\alpha^4 OH^-}{f_4} + \frac{\beta_{68}\,\alpha^6 Pb^{2+}\,\alpha^8 OH^-}{f_4} + \frac{\beta_{c11}\,\alpha Pb^{2+}\,\alpha CO_3^{2-}}{f_0} + \frac{\beta_{c12}\,\alpha Pb^{2+}\,\alpha^2 CO_3^{2-}}{f_2} \quad (7)$$

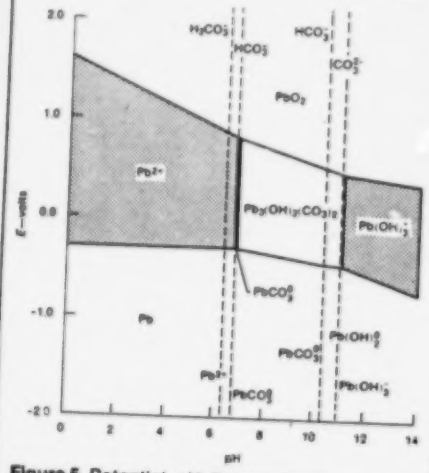

Figure 5. Potential–pH diagram for $C_t = 10^{-3.7}$ *M* (20 mg/L as $CaCO_3$) and dissolved Pb(II) species concentrations of 10^{-6} *M* (0.21 mg/L)

I = 0; temperature = 25° C; areas of passivation and immunity are unshaded.

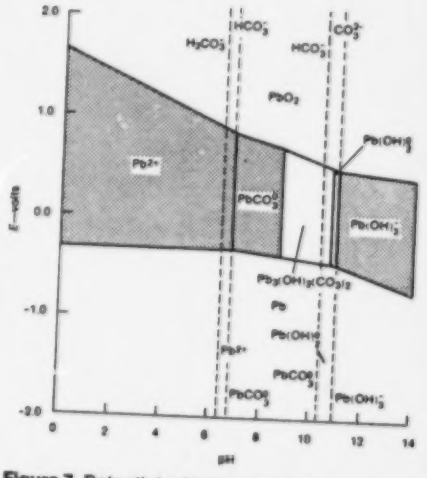

Figure 7. Potential–pH diagram for $C_t = 10^{-3.7}$ *M* (20 mg/L as $CaCO_3$) and dissolved Pb(II) species concentrations of $10^{-3.62}$ *M* (0.05 mg/L)

I = 0; temperature = 25° C; areas of passivation and immunity are unshaded.

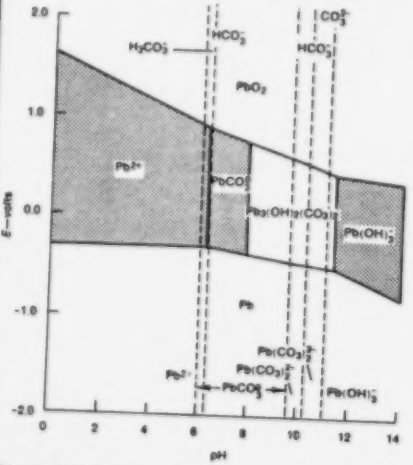

Figure 6. Potential–pH diagram for $C_t = 10^{-2.7}$ *M* (200 mg/L as $CaCO_3$) and dissolved species concentrations of $10^{-4.0}$ *M* (0.21 mg/L)

I = 0; temperature = 25° C; areas of passivation and immunity are unshaded.

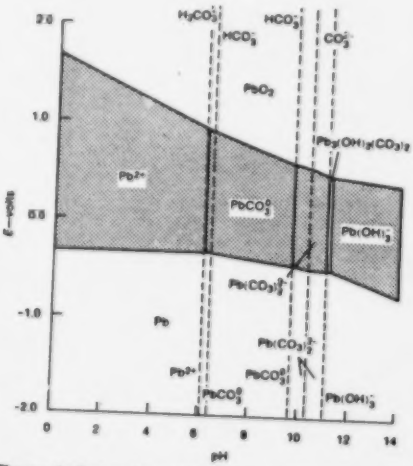

Figure 8. Potential–pH diagram for $C_t = 10^{-2.7}$ *M* (200 mg/L as $CaCO_3$) and dissolved Pb(II) species concentrations of $10^{-3.62}$ *M* (0.05 mg/L)

I = 0; temperature = 25° C; areas of passivation and immunity are unshaded.